

Alternative electron transport layer based on Al-doped ZnO and SnO₂ for perovskite solar cells: impact on microstructure and stability

Manon SPALLA ^{a,b}, Emilie PLANES ^{a,}, Lara PERRIN ^a, Muriel MATHERON ^b, Solenn BERSON ^b, Lionel FLANDIN ^a*

^a Univ. Grenoble Alpes, Univ. Savoie Mont Blanc, CNRS, Grenoble INP, LEPMI, 38000 Grenoble, France

^b Univ. Grenoble Alpes, CEA, LITEN, INES, 73375 Le Bourget du Lac, France

**emilie.planes@univ-smb.fr*

Supporting Information









	10s	1min	10min	35min	60min
AZO					
SnO ₂					

Figure S1: Photographs of substrates showing the influence of the annealing time (100°C) for the perovskite layer formation and decomposition depending on the ETL underlying layer used (AZO or SnO₂) – red squares indicate chosen optimized conditions.

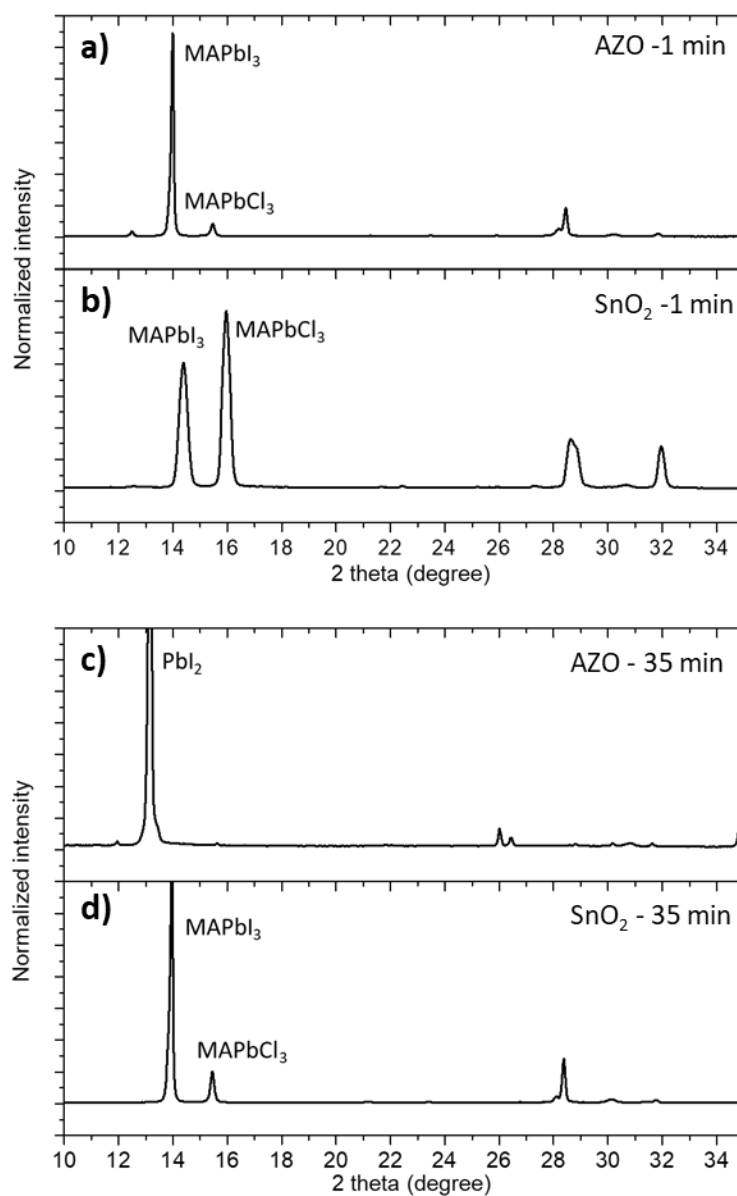


Figure S2: XRD diffractograms of perovskite annealed at 100°C : for 1 min on a) AZO and b) SnO_2 and for 35 min on c) AZO and d) SnO_2 (intensity normalized with ITO).

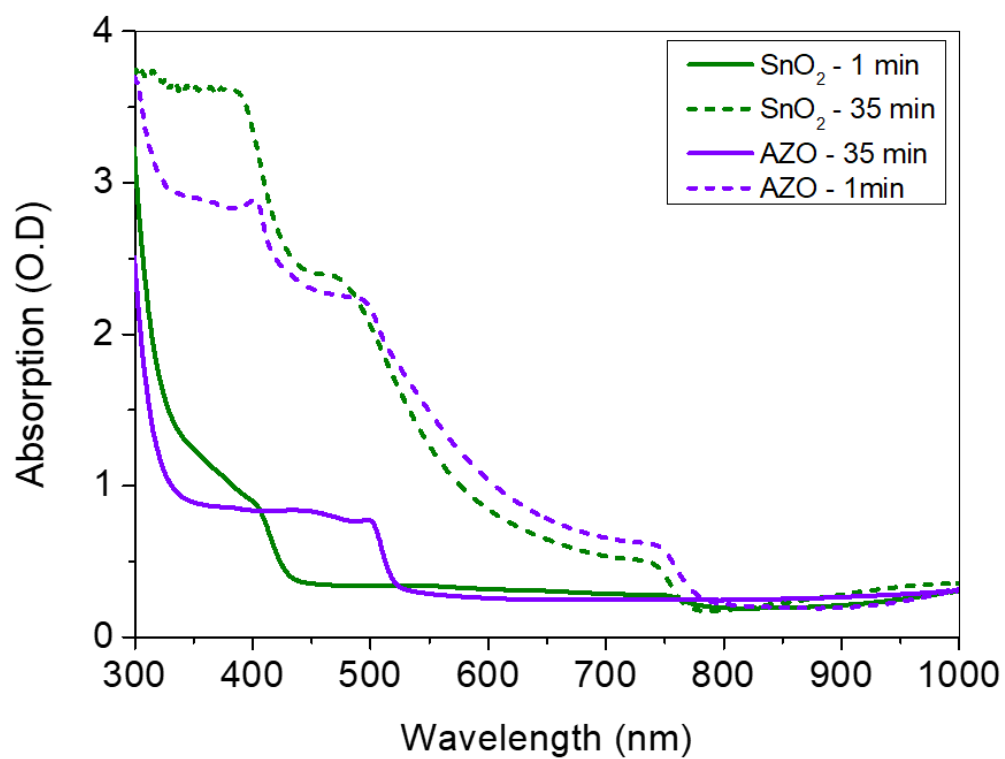


Figure S3: UV-visible absorption spectra of perovskite on AZO and SnO₂ layers after 100°C annealing for both 1 and 35 min.

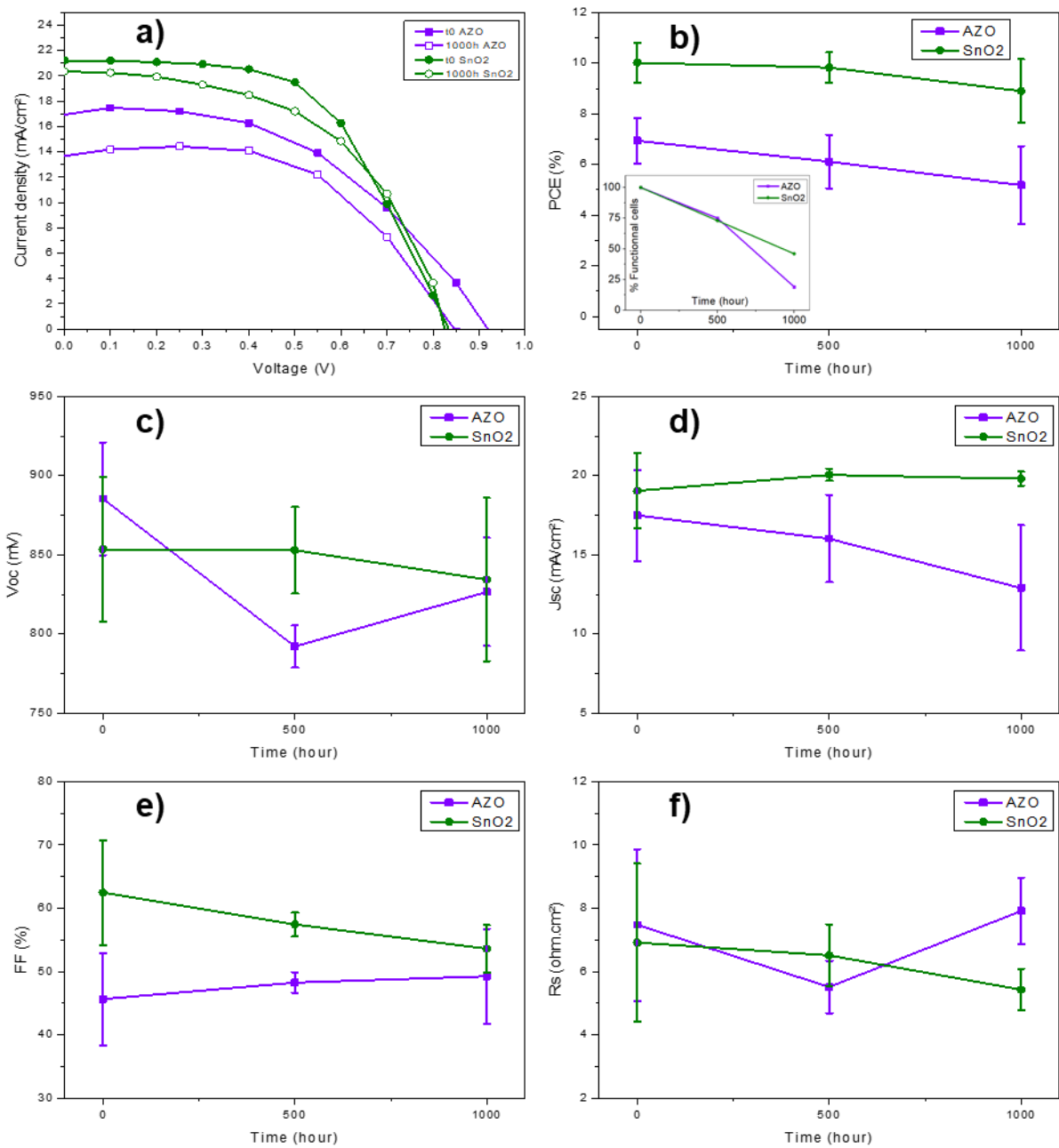


Figure S4: a) J-V curves for both architectures before and after 1000 h aging; b) PCE (%) for functional cells and quantification (%) of remaining functional cells; c) V_{oc} (mV), d) J_{sc} ($\text{mA}\cdot\text{cm}^{-2}$), e) FF (%) and f) R_s ($\text{ohm}\cdot\text{cm}^2$) parameters for both architectures during aging campaigns.

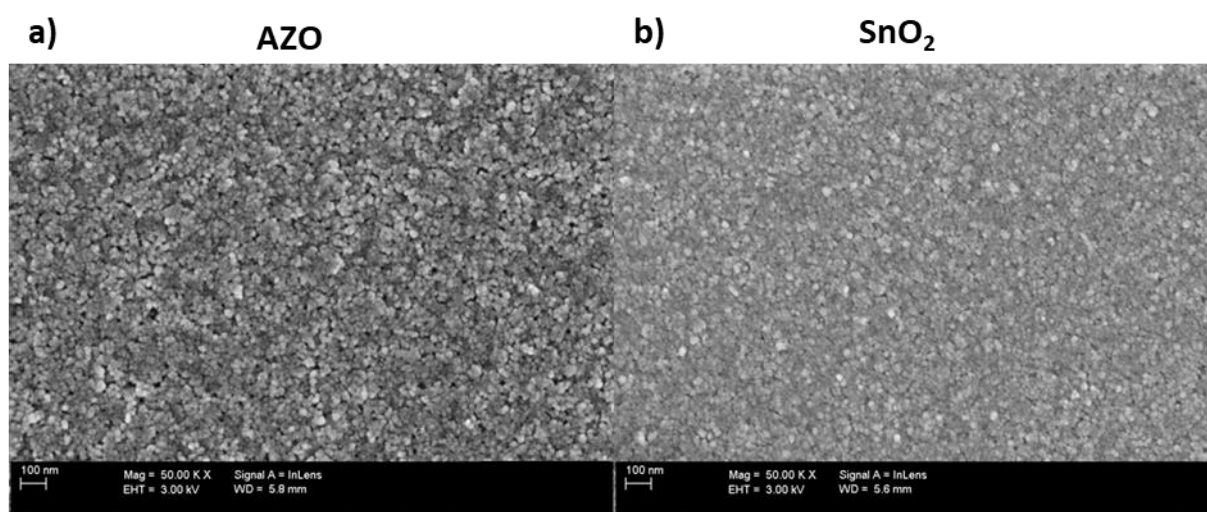
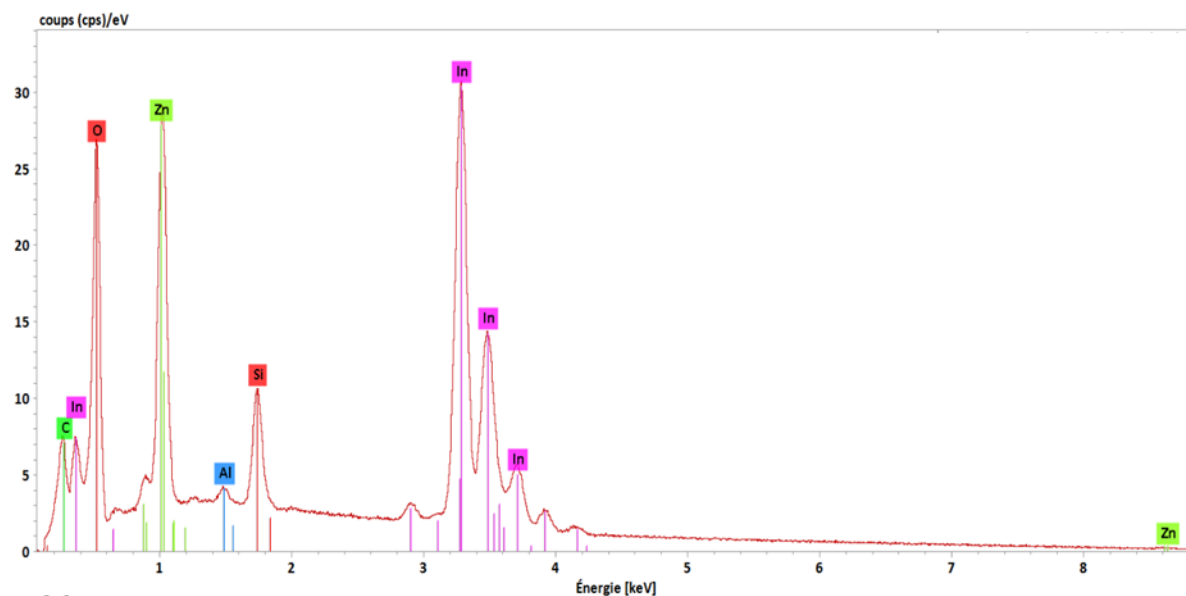


Figure S5: SEM surface images of a) AZO and b) SnO₂ layers.

a) AZO



b) SnO₂

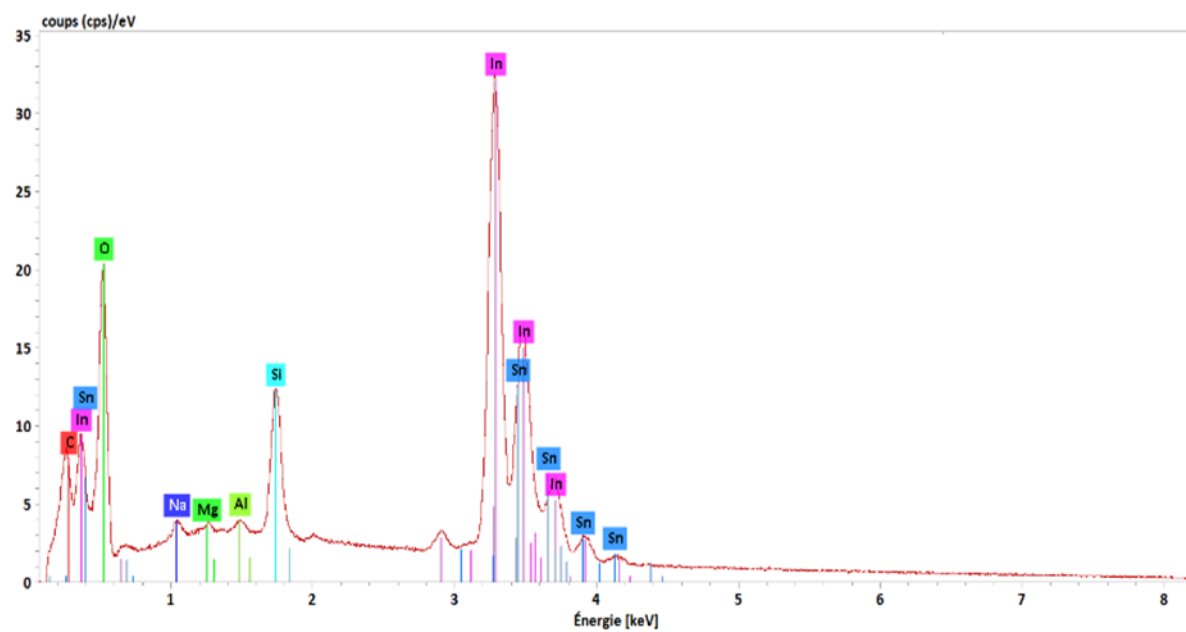


Figure S6: EDX analyses of a) AZO and b) SnO₂ layers.

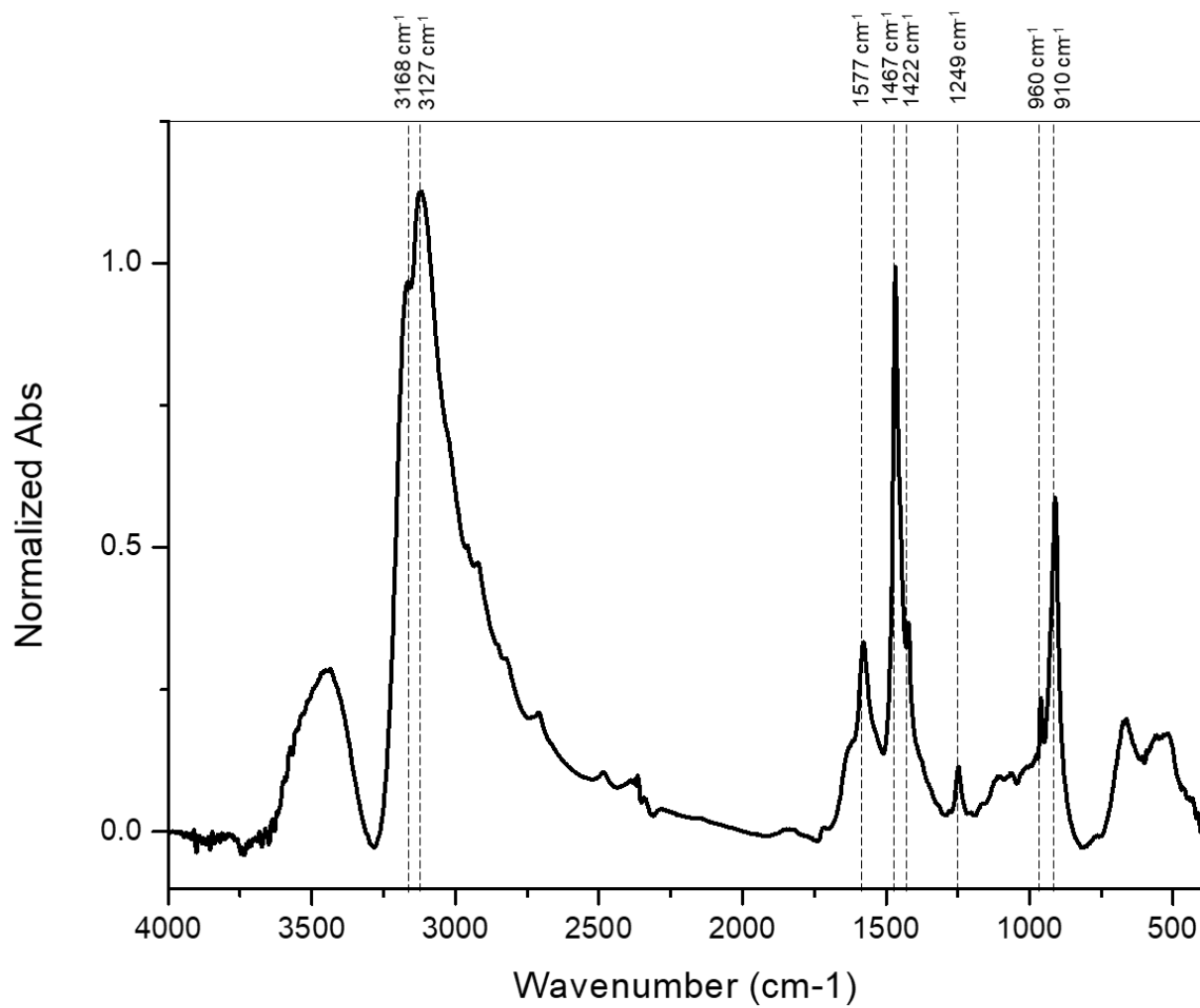


Figure S7: Full range FTIR spectrum of a MAPbI_{3-x}Cl_x layer (on SnO₂) with bands assignment.

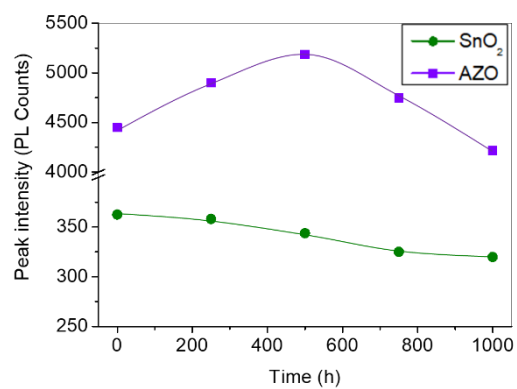


Figure S8: Variation of PL intensity with aging time on both AZO and SnO₂ perovskite half cells.

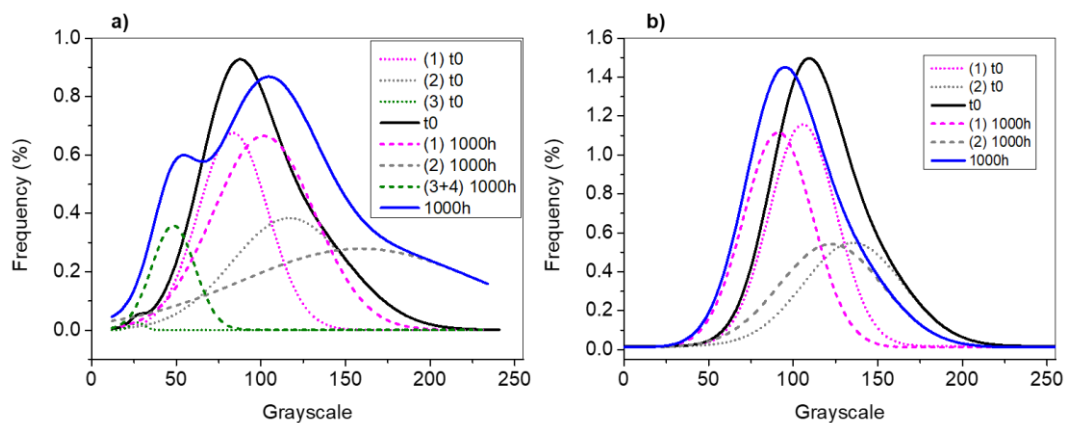


Figure S9: Evolution with time of the grayscale distribution of SEM images on both (a) AZO and (b) SnO₂ systems.

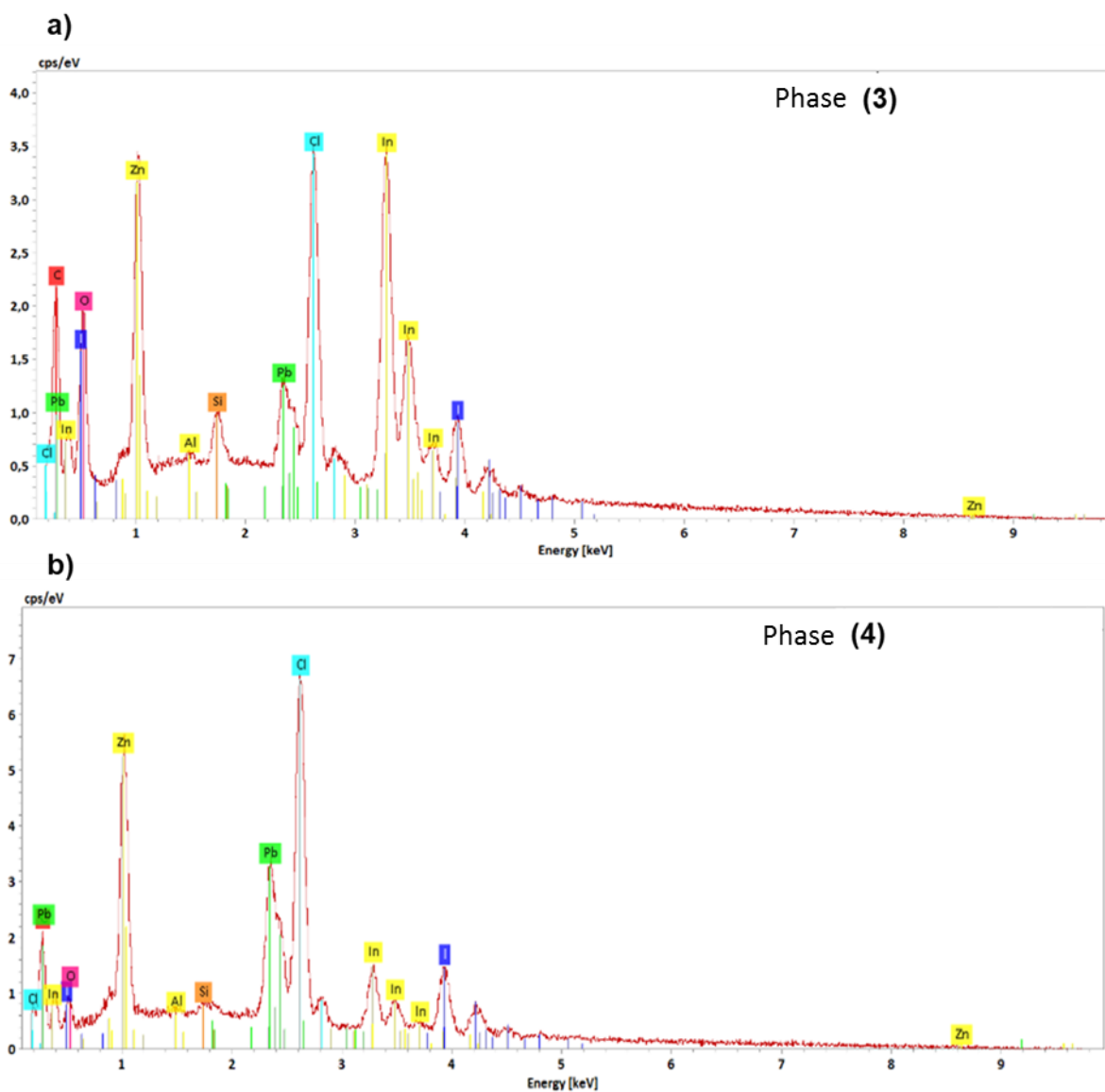


Figure S10: Raw EDS spectra with precise attributions for phases a) (3) and b) (4)

	Time (hour)	Voc (mV)	Jsc (mA/cm ²)	FF (%)	PCE (%)	Rs (ohm.cm ²)
AZO	0	885 ± 36	17.4 ± 2.9	46 ± 7	6.9 ± 0.9	7.4 ± 2.4
	500	792 ± 13	16 ± 2.8	48 ± 2	6.1 ± 1.1	5.5 ± 0.8
	1000	826 ± 34	12.9 ± 4.0	49 ± 7	5.2 ± 1.5	7.9 ± 1.1
SnO ₂	0	853 ± 46	19 ± 2.4	62 ± 8	10 ± 0.8	6.9 ± 2.5
	500	853 ± 27	20 ± 0.4	57 ± 2	9.8 ± 0.6	6.5 ± 1.0
	1000	834 ± 52	19.8 ± 0.5	53 ± 4	8.9 ± 1.3	5.4 ± 0.7

Table S1: PV parameters for both architectures during aging tests.

Wavenumbers (cm ⁻¹)	Peaks assignment
910	CH ₃ - NH ₃ ⁺ rock v ₁₂
960	C – N stretch v ₅
1249	CH ₃ - NH ₃ ⁺ rock v ₁₁
1376	Sym. CH ₃ bend v ₄
1422	Asym. CH ₃ bend v ₁₀
1467	Sym. NH ₃ ⁺ bend v ₃
1577	Asym. NH ₃ ⁺ bend v ₉
3127	Sym NH ₃ ⁺ stretch v ₁
3168	Asym NH ₃ ⁺ stretch v ₇

Table S2: Assignment of MAPbI_{3-x}Cl_x FTIR vibration bands.

Material	Orientation	Position (°)
PbI ₂		12.46
MAPbI ₃	(110) (002)	13.94
MAPbCl ₃	(100)	15.46
ITO		21.30
PbCl ₂		23.47
PbI ₂		25.89
MAPbI ₃	(220) (004)	28.19 ; 28.39
ITO		30.24
MAPbCl ₃	(200)	31.86

Table S3: XRD peaks assignment (according Cu source equivalent values).

		(1) MAPbI _{3-x} Cl _x	(2) MAPbI _{3-x} Cl _x + PbI ₂	(3) MACl + porosity	(4) PbX ₂ + porosity
AZO	t0	52 %	46 %	2 %	
	1000h	45 %	45 %	10 %	
SnO ₂	t0	100%			
	1000h	100%			

Table S4: Repartition of the different identified phases depending on both aging time and ETL layer nature, determined according to the surface grayscale analysis of SEM images (see Figure S9) and EDS analyses.